

# Convergent Cross-Mapping and Causality Detection

McCracken, Weigel

June 15, 2014

## Abstract

Convergent Cross-Mapping is a technique, introduced by Sugihara *et al.* [19], reported to be “a necessary condition for causation” capable of distinguishing causality from correlation in sets of time series data. We will show that CCM correlations do not in general agree with intuitive concepts of “driving” and “response”, and as such, relationships among CCM correlations should not be considered indicative of causality. It is shown that the calculation of CCM correlations can, however, be modified to identify asymmetric relationships between pairs of time series data. We introduce “pairwise asymmetric inference” (PAI) and present examples of its use in inferring relationships within complex systems. The sensitivity of CCM correlations on embedding dimensions and lag times will be discussed.

## 1 Introduction

Modern time series analysis includes a handful of techniques meant to discern “driving” or “cause and effect” relationships between different data sets. These techniques have found application in a wide range of fields including neuroscience (e.g. [8]), economics (e.g. [3, 2]), climatology (e.g. [13]), and others. General casual relationships in time series data are also being studied in an effort to understand causality itself (e.g. [4]).

To date, most techniques for “causal inference” in time series data fall into two broad categories, those related to transfer entropy and those related to Granger causality. Transfer entropy (introduced in [15]) and Granger causality (introduced in [5]) are known to be equivalent under certain conditions [1]. In this article, we investigate a casual inference technique, called Convergent cross-mapping (CCM), that was recently introduced by Sugihara *et al.* in [19]. Currently, there is no evidence that CCM is related to either transfer entropy or Granger causality.

We will begin with a review of the work of Sugihara *et al.*, including working through the coupled logistic map example presented in [19]. We will then illustrate the dependence of CCM correlations on the embedding dimension and lag time parameters of the CCM algorithm. Finally, we will introduce “pairwise asymmetric inference” (PAI) and use it to show that, even

though CCM causality may not be physical causality, it can still be a useful tool in the analysis of complex time series data.

## 2 Convergent Cross-Mapping

CCM is described as a technique used to identify “causality” between time series and is intended to be useful in situations where Granger causality is known to be invalid (i.e. in dynamic systems that are “non-seperable” [19]). The authors state that CCM is a “necessary condition for causation”. It is well known [6, 10, 14] that Granger causality is not causality as it is typically understood in physics. It will be shown that a similar conclusion can be drawn regarding CCM causality.

CCM is closely related to simplex projection [18, 17], which predicts a point in the times series  $X$  at a time  $t + 1$ , i.e.  $X_{t+1}$ , by using the points with the most similar histories to  $X_t$ . Similarly, CCM uses points with the most similar histories to  $X_t$  to estimate  $Y_t$ . The CCM correlation is the squared correlation coefficient<sup>1</sup> between the original time series  $Y$  and estimate of  $Y$  made using the convergent cross-mapping with  $X$ , which is labeled as  $Y|X$ ; i.e. the CCM correlation is given as

$$C_{YX} = (\rho(Y, Y|X))^2,$$

where  $\rho(A, B)$  is the Pearson correlation coefficient between  $A$  and  $B$  []. Any pair of times series,  $X$  and  $Y$ , will have two CCM correlations,  $C_{YX}$  and  $C_{XY}$ , which are compared to determine the CCM causality. For example, Sugihara *et al.* define a difference of CCM correlations

$$\Delta = C_{YX} - C_{XY} \quad (1)$$

and use the sign of  $\Delta$  to determine the CCM causality between  $X$  and  $Y$  [19]. The CCM algorithm is explained in more detail in Appendix 8.

If  $X$  can be estimated from the shadow manifold of  $Y$  better than  $Y$  can be estimated from the shadow manifold of  $X$  (e.g. if  $\Delta < 0$ ), then  $X$  is said to “CCM cause”  $Y$ .

<sup>1</sup>This definition differs slightly from the original definition in [19], which just uses Pearson’s correlation coefficient. We use the square of this value to avoid dealing with negative correlation values. This subtle change in the definition does not affect the conclusions drawn in [19], as can be seen in our reproduction of key plots from that work.

## 2.1 Simplified Two Population Dynamics

Consider the example system used by Sugihara *et al.* in [19]:

$$X_t = X_{t-1}(r_x - r_x X_{t-1} - \beta_{xy} Y_{t-1}) \quad (2)$$

$$Y_t = Y_{t-1}(r_y - r_y Y_{t-1} - \beta_{yx} X_{t-1}) \quad (3)$$

where  $r_x, r_y, \beta_{xy}, \beta_{yx} \in \mathbf{R} \geq 0$ . This pair of equations is a specific form of the two-dimensional coupled logistic map system, which is known to be chaotic [11].

In this example, the CCM causality of this system is determined by sampling both the initial conditions and the dynamics parameters, calculating  $\Delta$ , and demonstrating the necessary convergence. The dynamic parameters  $r_x$  and  $r_y$  are sampled from a normal distributions  $N(\mu_{rx}, \sigma_{rx})$  and  $N(\mu_{ry}, \sigma_{ry})$ , respectively. The initial conditions  $X_0$  and  $Y_0$  are also sampled from normal distributions, specifically  $N(\mu_{x0}, \sigma_{x0})$  and  $N(\mu_{y0}, \sigma_{y0})$ . The coupling parameters  $\beta_{xy}$  and  $\beta_{yx}$  are then varied over the interval  $[10^{-6}, 1]$  (in steps of 0.02) to produce the plots seen in Figure ??.

Sugihara *et al.* consider convergence to be critically important to determining CCM causality, identifying it as “a key property that distinguishes causation from simple correlation” [19]. Figure ?? shows plots created with several different library lengths to illustrate the convergence of  $\Delta$  for this example. Typically, for convenience, the (approximately) converged CCM correlation values will be reported and proof of convergence will be implied, rather than shown.

(a) (b)

(c) (d)

Figure 1: These plots show the dependence of Eqn. 1 on  $\beta_{xy}$  and  $\beta_{yx}$ . See the text for details on how these plots were created along with a discussion of the interpretation of these plots in terms of CCM causality.

The idea is that  $\beta_{xy} > \beta_{yx}$  intuitively implies  $Y$  “drives”  $X$  more than  $X$  “drives”  $Y$ . Stated more formally,  $\beta_{xy} > \beta_{yx} \Rightarrow \Delta > 0$ , which is reported as “ $Y$  CCM causes  $X$ ”. Likewise,  $\beta_{xy} < \beta_{yx}$  implies  $X$  CCM causes  $Y$  and  $\beta_{xy} = \beta_{yx}$  implies no CCM causality in the system. It will be shown below that CCM causality is not necessarily related to causality as it is typically understood in physics.

## 3 Embedding Dimension and Lag Time

The CCM algorithm depends on the embedding dimension  $E$  and the lag time step  $\tau$  (see Appendix 8). Consider the simplified two population system (Eqn.

2) with  $r_x = 3.8$ ,  $r_y = 3.5$ ,  $\beta_{xy} = 0.01$ ,  $\beta_{yx} = 0.2$ ,  $X_0 = 0.4$ , and  $Y_0 = 0.2$  with  $X$  and  $Y$  library lengths of  $L = 2000$ . Figure ?? shows the effect of varying  $E$  and  $\tau$  on  $\Delta$  for this system.  $E$  is varied over the interval  $[2, 20]$  (in steps of 1), and  $\tau$  is varied over the interval  $[1, 50]$  (also in steps of 1). This figure makes it clear that a statement of CCM causality (and, subsequently, that statement’s agreement with intuition) depends strongly upon how the CCM technique is used. A dependence  $E$  and  $\tau$  is a feature of most state space

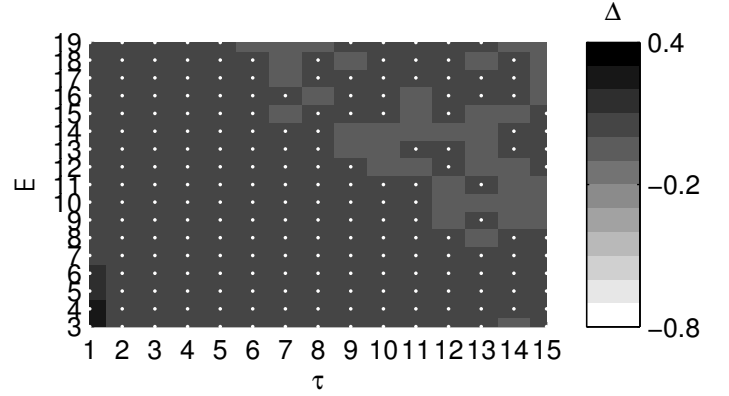


Figure 2: The determination of CCM causality in a system is dependent on the CCM parameters of embedding dimension  $E$  and lag time step  $\tau$ . This plot show the dependence of Eqn. 1 on  $E$  and  $\tau$  for the example system discussed in the text. The white dots indicate  $\Delta < 0$ .

reconstruction (SSR) methods [12, 20, 16]. CCM is related to state space reconstruction [19], so the  $E$  and  $\tau$  dependence seen here is not unexpected. Sugihara *et al.* do not discuss in depth how to determine  $E$  and  $\tau$ , but they do mention that “optimal embedding dimensions” are found using univariate SSR [19] (supplementary material). Other methods for determining  $E$  and  $\tau$  for SSR algorithms can be found in the literature (e.g. [12, 16, 9]).

## 4 Simple Example Systems

The usefulness of the CCM algorithm in identifying causal or driving structure among sets of time series can be explored by using simple example systems. Each of the following examples intuitively supports the conclusion that  $X$  drives  $Y$ , and applying the CCM algorithm (with  $E = 3$  and  $\tau = 1$ ) leads to conclusions that do not always agree with this intuition.

### 4.1 Linear Example

Consider the linear example dynamical system of

$$X_t = \sin(t) \quad (4)$$

$$Y_t = AX_{t-1} + B\eta_t, \quad (5)$$

with  $A, B \in \mathbb{R} \geq 0$  and  $\eta_t \sim \mathcal{N}(0, 1)$ . Specifically, consider  $A, B \in [0, 10]$  in increments of 0.1. Figure 3 shows  $\Delta$  for this example given a library length of  $L = 2000$ . The convergence of two specific points in

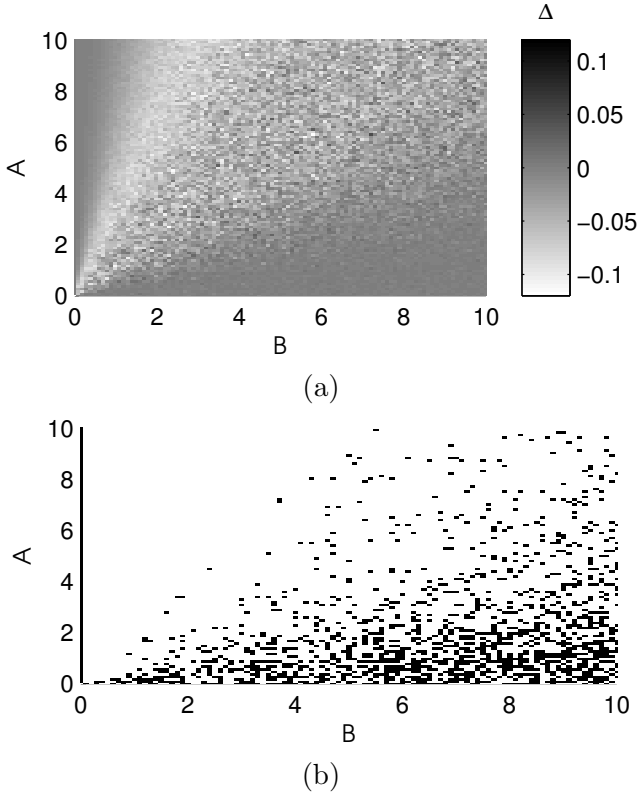


Figure 3: The sign of  $\Delta$ , and thus the CCM causality, depends on  $A$  and  $B$ . (a)  $\Delta$  calculated as described in the text; (b) Two color version of (a) where black indicates  $\Delta > 0$  and white indicates  $\Delta < 0$ .

Figure 3,  $(A, B) = (2.6, 2.6)$  and  $(A, B) = (3.0, 2.6)$ , are shown in Figure 4.

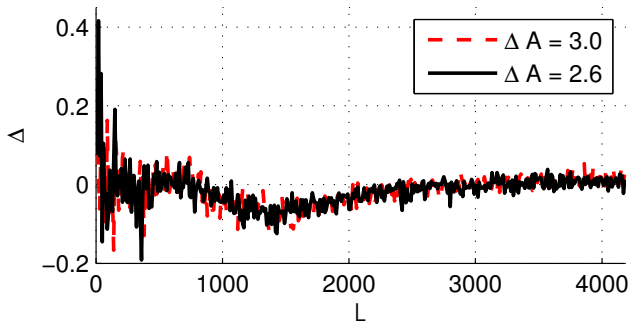


Figure 4: The convergence of points  $(A, B) = (2.6, 2.6)$  and  $(A, B) = (3.0, 2.6)$  from Figure 3.

The expected conclusion of  $X$  drives  $Y$  would correspond to  $X$  CCM causes  $Y$ , which implies  $\Delta < 0$ . But, it can be seen from the plots above that the sign of  $\Delta$  changes as  $A$  and  $B$  change. Given that the intuitive conclusion of  $X$  drives  $Y$  in Eqn. 4 does not depend

on  $A$  and  $B$ , it would seem that  $\Delta$  does not reliably reflect the intuitive conclusion in this linear example system.

Figure 4 shows (for the two specific points plotted) that  $\Delta$  is more negative at shorter library lengths but appears to converge to a point near zero as the library length is increased. The convergence of CCM correlations is emphasized [19], so the seemingly counter intuitive behavior of  $\Delta$  (and  $C_{XY}$  and  $C_{YX}$ ) in Figure 4 again seems to imply that the CCM correlations may not be a reliable measure of “driving” (at least not the intuitive definition) for this simple linear example system.

## 4.2 Non-Linear Example

Consider the non-linear example dynamical system of

$$X_t = \sin(t) \quad (6)$$

$$Y_t = AX_{t-1}(1 - BX_{t-1}) + C\eta_t, \quad (7)$$

with  $A, B, C \in \mathbb{R} \geq 0$  and  $\eta_t \sim \mathcal{N}(0, 1)$ . Specifically, consider  $A, B, C \in [0, 5]$  in increments of 0.5. Figure 5 shows  $\Delta$  for specific values of  $C$  given a library length of  $L = ??$ . Just as in the previous linear example, the

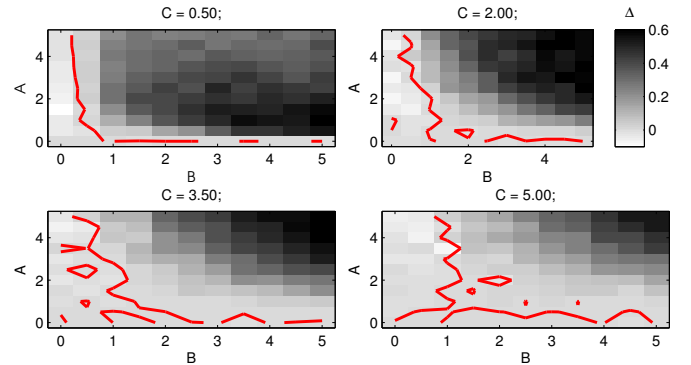


Figure 5

expectation for this example system is that  $\Delta < 0$  independent of the parameters  $A$ ,  $B$ , and  $C$ . However, it can be seen from the plots that the sign of  $\Delta$  can depend on all three parameters. Thus this simple non-linear example leads to a similar conclusion to the previous linear example; i.e.  $\Delta$  does not appear to reliably reflect intuitive notions of driving.

## 5 RL Circuit Example

Both of the previous examples included a noise term,  $\eta_t$  (which was not averaged over in any way). The failure of CCM correlations to meet expectations in the previous examples may be considered a failure of the algorithm’s ability to deal with noise. This idea can be investigated by considering a system without stochastic noise terms. To that end, consider the familiar physical

system of a electrical circuit containing a resistor and an inductor.

The continuous system is

$$\frac{dI}{dt} = \frac{V(t)}{L} - \frac{R(t)}{L}I, \quad (8)$$

where  $I$  is the current at time  $t$ ,  $V(t)$  is the voltage at time  $t$ ,  $R(t)$  is the resistance at time  $t$ , and  $L$  is the inductance (which is also constant in these examples), and it can be approximated as

$$\dot{I} = \frac{V(t)}{L} - \frac{R(t)}{L}I \Rightarrow I_{t+1} - I_t = \frac{V_t}{L} - \frac{R_t}{L}I_t. \quad (9)$$

Rearranging leads to

$$I_{t+1} = \frac{V_t}{L} + I_t \left(1 - \frac{R_t}{L}\right), \quad (10)$$

$$V_t = L \left( I_{t+1} - I_t \left(1 - \frac{R_t}{L}\right) \right), \quad (11)$$

and

$$R_t = L \left( I_t - I_{t+1} + \frac{V_t}{L} \right). \quad (12)$$

All of the plots of  $I$  seen below are produced by using MATLAB's *ode45* to solve Eqn. 8 (i.e. not using the discrete approximation shown). The time series  $V(t)$  and  $R(t)$  are created by defining values at fixed points and using linear interpolation (i.e. MATLAB's *interp1*) to find the time steps required by the ODE solver.

### 5.1 Changing $V(t)$

Consider the situation where  $L = 10H$  and  $R(t) = R_0 = 5\Omega$  is constant. Physical intuition is that  $V$  drives  $I$ , so we expect to find  $V$  CCM causes  $I$  (i.e.  $C_{VI} > C_{IV}$  or  $\Delta = C_{VI} - C_{IV} > 0$ ). For this example, the voltage is described by

$$V(t) = A_v \sin(t), \quad (13)$$

where  $A_v$  is the amplitude.

Consider evaluating the CCM correlations  $C_{VI}$  and  $C_{IV}$  for each  $A_v \in [0.01, 2.0]V$  in steps of  $0.01V$ . The CCM correlations are found using  $E = 3$  and  $\tau = 1$  and both are plotted in Figure 6 (along with  $\Delta$ ). It appears that  $\Delta$  does not consistently agree with intuition in this example either. Notice that, unlike the previous examples, there are no noise terms in this system.

The resistance and inductance of the circuit are fixed and the voltage is varied from  $1 \times 10^{-2}$  to 2.0 volts in discrete steps of 0.01 volts. This traditional experiment is straightforward to imagine. Physically changing the voltage and witnessing a resulting change in the current is enough to convince most people that the voltage “drives” the current. Rigorous statistical hypothesis testing can be performed to strengthen the confidence in such a conclusion. Yet, from Figure 6, it appears that the voltage does not consistently “CCM

cause” the current. Thus, it seems as though CCM causality does not agree with physical causality (at least for the specific RL circuit experiment described here).

It may be argued that the relatively small values (as compared to the previous examples) of  $\Delta$  plotted in Figure 6 indicate that the correct conclusion should be either 1. there is no CCM causality in the system or 2. CCM causality is not applicable to this system. Conclusion (1) conflicts with the intuitive notion of an RL circuit as a strongly driven system and conclusion (2) conflicts with identifying CCM causality has a general qualifier of “driving” in a dynamical systems.

## 6 PAI

Consider the example system of Eqn. 2 with  $r_y = r_y = 3.7$ ,  $X_0 = 0.2$ ,  $Y_0 = 0.4$ ,  $\beta_{xy} = 0$ , and  $\beta_{yx} = 0.32$ . These parameters correspond to Figure 3C and D of [19] (with  $E = 2$ ,  $\tau = 1$ , and  $L = 1000$ ). Plots of the correlation between  $X$  and  $X|Y$  (i.e.  $X$  estimated using the weights found from the shadow manifold of  $Y$ ), as well as,  $Y$  and  $Y|X$  are shown below.

This leads to  $\Delta = C_{YX} - C_{XY} \approx 0.11 - 0.97 = -0.86$ . Notice  $\Delta < 0$  implies  $X$  CCM causes  $Y$ , which agrees with intuition because  $\beta_{xy} = 0 < \beta_{yx} = 0.32$ .

But, the correlations shown in Figure 7 are not the only correlations that can be tested. Consider, for example, the correlation between  $X$  and the corresponding  $X|X$ , which is estimated using weights found from the shadow manifold of  $X$  itself. The time series  $X$  may also be estimated using a multivariate shadow manifold consisting of points from both  $X$  and  $Y$ . For example, an  $E + 1$  dimensional point in the a multivariate shadow manifold constructed using both  $X$  and  $Y$  may be defined as  $\vec{X}_t = (X_t, X_{t-\tau}, X_{t-2\tau}, \dots, X_{t-(E-1)\tau}, Y_t)$ . An estimate of  $X$  using weights from a shadow manifold using that specific construction will be referred to as  $X|(XY)$ . See Figure 8.

A difference in CCM correlations similar to  $\Delta$  can be defined using the multivariate embedding. Consider  $\Delta' = C_{Y(YX)} - C_{X(XY)}$ . It might be argued, in close parallel to the arguments given in [19] for  $\Delta$ , that an intuitive definition of “driving” might be captured by the sign of  $\Delta'$ . For example, if  $\Delta' < 0$ , then the single time step of  $Y$  added to the delay vectors constructed from  $X$  create stronger estimators of  $X$  than the single time step of  $X$  added to the delay vectors constructed from  $Y$  do for  $Y$ . Thus, it might be argued, that  $Y$  contains more “information” about  $X$ , which leads to the conclusion  $X$  drives  $Y$  (this logic is very similar to that

given for  $\Delta$  in [19]). The example system and parameters (including  $E$ ,  $\tau$ , and  $L$ ) described at the beginning of this section leads to  $\Delta' \approx -3 \times 10^{-4}$  which agrees with the previously discussed conclusions of “ $X$  CCM causes  $Y$ ” and “ $X$  drives  $Y$ ”. Using the multivariate embedding described above to explore “driving” relationships between pairs of time series will be referred to as *pairwise asymmetric inference* or *PAI*.

Consider a comparison of PAI and CCM given the linear example system from above, i.e. Eqn. 4. Figure 9 plots  $\Delta'$  as a function of  $A$  and  $B$  using of the same  $E$ ,  $\tau$ ,  $L$ , and step sizes as was used to produce Figure 3.  $\Delta' < 0 \forall A, B$  in the domains shown in the figure. Thus, it appears  $\Delta'$  is in agreement with an intuitive definition of driving more consistently than  $\Delta$ . Notice,  $\Delta'$  is significantly smaller than  $\Delta$ , which is expected since the correlation of  $X$  and  $Y$  with their “self estimation” counterparts of  $X|X$  and  $Y|Y$  are initially very high, even without the multivariate additions. But, if the concept of driving is determined solely on the sign of  $\Delta'$ , then, at least for the simple linear example presented here, PAI appears to be a consistent qualifier of “driving”.

Reproducing Figure 4 using PAI shows an apparent reduction in some of the erratic behavior seen in CCM. See Figure 10.

The conclusions that PAI agrees with intuition more consistently than CCM is also supported by the non-linear example system, Eqn. 6. Figure ?? plots  $\Delta'$  as a function of  $A$ ,  $B$  and  $C$  using of the same  $E$ ,  $\tau$ ,  $L$ , and step sizes as was used to produce Figure 5. Again in contrast to the CCM figure, PAI seems to agree with intuition for all the plotted values of  $A$ ,  $B$ , and  $C$  (i.e.  $\Delta' < 0 \forall A, B, C$  in the domains shown).

Finally, a comparison of PAI and CCM for the RL circuit example leads to similar conclusions. See Figure 12.

## 7 Conclusion

The examples presented in this article have shown that CCM and, more consistently, PAI can be used to indicate “driving” relationships that agree with intuition. Such information can be useful, but should not be confused with physical causality. However, even without notions of causality, PAI may be useful exploratory data analysis. For example, PAI may help guide the development of physical causality models (e.g. by suggesting future experiments) in scenarios involving a large collection of simultaneous time series measurements of different variables in a system but no *a priori* notions of causality in the system.

It should also be noted that the basic idea behind CCM may be useful in studying time series driving independently of the specific implementation using  $\Delta$  (or the sign of  $\Delta$ ). SSR methods are model-independent,

which may be seen as a benefit over the popular Granger causality measures.

PAI attempts to keep the benefits of CCM while making it slightly more robust. But, the given definition of  $\Delta'$  is not without its own difficulties. For example,  $\Delta'$  does not account for the differences between correlations between  $X$  and  $X|X$  and  $Y$  and  $Y|Y$ . Such differences may bias conclusions drawn from using  $\Delta'$  with proper care.

As a concrete example, consider the example system and parameters (including  $E$ ,  $\tau$ , and  $L$ ) described at the beginning of Section 6. The value  $\Delta' \approx -3 \times 10^{-4}$  was already discussed, but notice  $C_{YY} - C_{XX} \approx 1.5 \times 10^{-3}$ , indicating that  $Y$  is a better “self estimator” than  $X$  (though both  $C_{YY}, C_{XX} > 0.99$ ). How does this fact affect interpretations of the  $\Delta' < 0$  result, which was that  $X$  drives  $Y$ ? Such questions are still open. It may be argued that a different measure may be more suitable, such as  $\Delta'' = |C_{Y(YX)} - C_{YY}| - |C_{X(XY)} - C_{XX}|$ . For this example,  $\Delta'' \approx 3.9 \times 10^{-4}$ , which does not agree with intuition, despite the agreement of both  $\Delta$  and  $\Delta'$ . Studying driving relationships among time series sets using state space methods is still full of open questions.

## 8 Appendix A: CCM Algorithm

A description of this algorithm is also available in [19] (supplementary materials). It is elucidating to partition the CCM algorithm into five distinct (though related) steps:

1. Create the shadow manifold for  $X$ , called  $\tilde{X}$
2. Find the nearest neighbors to  $\tilde{X}_t$
3. Use the nearest neighbors to create weights
4. Use the weights to estimate  $Y$ , called  $Y|X$
5. Find the correlation between  $Y$  and  $Y|X$

The steps vary in complexity and are explained in more detail below.

### 8.1 Create $\tilde{X}$

Given an embedding dimension  $E$ , the shadow manifold of  $X$ , called  $\tilde{X}$ , is created by associating an  $E$ -dimensional vector to each point  $X_t$  that is constructed as  $\tilde{X}_t = (X_t, X_{t-\tau}, X_{t-2\tau}, \dots, X_{t-(E-1)\tau})$  (this vector is often called a “delay vector”). The first such vector is created at  $t = 1 + (E - 1)\tau \equiv t_s$  and the last is at  $t = L \equiv t_l$  where  $L$  is the time series length (or “library length”).

## 8.2 Find Nearest Neighbors

The minimum number of points required for a bounding simplex in an  $E$ -dimensional space is  $E + 1$  (find a non-Sugihara reference for this statement). Thus, the nearest neighbor search results is a set of distances  $\{d_1, d_2, \dots, d_{E+1}\}$  and an associated set of times  $\{t_1, t_2, \dots, t_{E+1}\}$  (where the subscript 1 denotes the closest neighbor, 2 denotes the next closest neighbor, and so on). The distances from  $\vec{X}_t$  are defined as

$$d_i = D(\vec{X}_t, \vec{X}_{t_i}) ,$$

where  $D(\vec{a}, \vec{b})$  is the Euclidean distance between vectors  $\vec{a}$  and  $\vec{b}$ .

## 8.3 Create Weights

Each nearest neighbor will be used to find an associated weight. The unnormalized weights are defined as

$$u_i = e^{-\frac{d_i}{d_1}} .$$

The weights are defined as

$$w_i = \frac{u_i}{N} ,$$

where the normalization factor is given as

$$N = \sum_j u_j .$$

## 8.4 Find $Y|X$

A point  $Y_t$  in  $Y$  can be estimated using the (normalized) distances to the points in  $X$  using the weights calculated above. This estimate is calculated as

$$Y_t|X = \sum_i w_i Y_{t_i} .$$

## 8.5 Find the Correlation

The CCM correlation is defined as

$$C_{YX} = (\rho(Y, Y|X))^2 ,$$

where  $\rho_{A,B}$  is the standard Pearson's correlation coefficient between  $A$  and  $B$ . It can be seen from the above algorithm that  $X = Y \Rightarrow C_{YX} = C_{XY}$ , but in general,  $C_{YX} \neq C_{XY}$ .

## References

- [1] Lionel Barnett, Adam B. Barrett, and Anil K. Seth. Granger causality and transfer entropy are equivalent for gaussian variables. *Phys. Rev. Lett.*, 103:238701, Dec 2009.
- [2] Jean-Marie Dufour, Denis Pelletier, and Éric Renault. Short run and long run causality in time series: inference. *Journal of Econometrics*, 132(2):337–362, 2006.
- [3] Jean-Marie Dufour and Eric Renault. Short run and long run causality in time series: theory. *Econometrica*, pages 1099–1125, 1998.
- [4] Michael Eichler and Vanessa Didelez. Causal reasoning in graphical time series models. *arXiv preprint arXiv:1206.5246*, 2012.
- [5] Clive WJ Granger. Investigating causal relations by econometric models and cross-spectral methods. *Econometrica: Journal of the Econometric Society*, pages 424–438, 1969.
- [6] C.W.J. Granger. Testing for causality: A personal viewpoint. *Journal of Economic Dynamics and Control*, 2(0):329 – 352, 1980.
- [7] D. Halliday, R. Resnick, and J. Walker. *Fundamentals of Physics Extended, 10th Edition*. Wiley Global Education, 2013.
- [8] Maciej Kaminski, Mingzhou Ding, Wilson A. Truccolo, and Steven L. Bressler. Evaluating causal relations in neural systems: Granger causality, directed transfer function and statistical assessment of significance. *Biological Cybernetics*, 85(2):145–157, 2001.
- [9] Matthew B. Kennel, Reggie Brown, and Henry D. I. Abarbanel. Determining embedding dimension for phase-space reconstruction using a geometrical construction. *Phys. Rev. A*, 45:3403–3411, Mar 1992.
- [10] Yan Liu and Mohammad Taha Bahadori. A survey on granger causality: A computational view. *University of Southern California*, <http://www-bcf.usc.edu/~liu32/granger.pdf> (12. 03.2013), 2012.
- [11] Alun L. Lloyd. The coupled logistic map: a simple model for the effects of spatial heterogeneity on population dynamics. *Journal of Theoretical Biology*, 173(3):217 – 230, 1995.
- [12] Hong-guang Ma and Chong-zhao Han. Selection of embedding dimension and delay time in phase space reconstruction. *Frontiers of Electrical and Electronic Engineering in China*, 1(1):111–114, 2006.
- [13] Timothy J Mosedale, David B Stephenson, Matthew Collins, and Terence C Mills. Granger causality of coupled climate processes: Ocean feedback on the north atlantic oscillation. *Journal of climate*, 19(7), 2006.

- [14] David L. Roberts and Stephen Nord. Causality tests and functional form sensitivity. *Applied Economics*, 17(1):135–141, 1985.
- [15] Thomas Schreiber. Measuring information transfer. *Phys. Rev. Lett.*, 85:461–464, Jul 2000.
- [16] Michael Small and C.K. Tse. Optimal embedding parameters: a modelling paradigm. *Physica D: Nonlinear Phenomena*, 194(3–4):283 – 296, 2004.
- [17] G. Sugihara and R. M. May. Nonlinear forecasting as a way of distinguishing chaos from measurement error in time series. *Nature*, 344:734–741, April 1990.
- [18] George Sugihara, Bryan Grenfell, Robert M. May, P. Chesson, H. M. Platt, and M. Williamson. Distinguishing error from chaos in ecological time series [and discussion]. *Philosophical Transactions of the Royal Society of London. Series B: Biological Sciences*, 330(1257):235–251, 1990.
- [19] George Sugihara, Robert May, Hao Ye, Chih-hao Hsieh, Ethan Deyle, Michael Fogarty, and Stephan Munch. Detecting causality in complex ecosystems. *Science*, 338(6106):496–500, 2012.
- [20] I Vlachos and D Kugiumtzis. State space reconstruction from multiple time series. In *Topics on Chaotic Systems: Selected Papers from Chaos 2008 International Conference*, page 378. World Scientific, 2009.

Figure 6: Changing  $A_v$ .

- (a) Correlation between  $X$  and  $X|Y$
- (b) Correlation between  $Y$  and  $Y|X$

Figure 7: Reproductions of Figures 3C and 3D from [19].

- (a) Correlation between  $X$  and  $X|X$
- (b) Correlation between  $X$  and  $X|(XY)$
- (c)  $C_{XX}$
- (d)  $C_{X(XY)}$

Figure 8: Stronger correlations, as compared to Figure 7, can be seen between a time series and its estimate when the shadow manifold includes points from the time series it is estimating. See the text for more details.

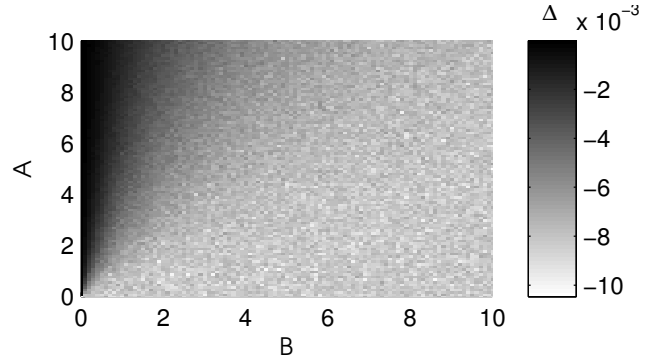


Figure 9: Reproducing Figure 3 using PAI rather than CCM. Notice that  $\Delta' < 0 \forall A, B$  implying  $X$  “PAI drives”  $Y$ .

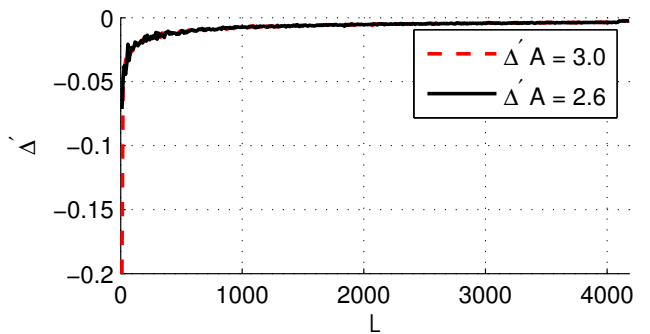


Figure 10: Reproducing Figure 3 using PAI rather than CCM. Notice that  $\Delta'$  does not display the apparent erratic behavior seen in  $\Delta$  in Figure 3.

Figure 11: Non Linear Example PAI

Figure 12: Changing  $A_v$ .